Inorganic Chemistry

Article

pubs.acs.org/IC

Tris(β-diketonato) Ru(III) Complexes as Chiral Dopants for Nematic Liquid Crystals: the Effect of the Molecular Structure on the Helical Twisting Power

Jun Yoshida,*[,†] Go Watanabe,[‡] Kaori Kakizawa,[†] Yasuhiro Kawabata,[†] and Hidetaka Yuge[†]

[†]Department of Chemistry and [‡]Department of Physics, School of Science, Kitasato University, 1-15-1 Kitasato, Minami-ku, Sagamihara, Kanagawa 252-0373, Japan

Supporting Information

ABSTRACT: Doping nematic liquid crystals with optically active compounds transforms them into chiral nematic phases with helical structures. In this phenomenon, the chirality of the dopant molecules is transferred or amplified to the bulk of the liquid crystals. Δ-[Ru(acac)$_3$] (acac = acetylacetonato) is known to work as one of the dopants with a strong helical twisting power (HTP). In this study, we have systematically modified [Ru(acac)$_3$] to clarify the correlation between the molecular structure and HTP; we have designed and synthesized five new Ru(III) complexes, [Ru(acac)$_2$(acacC$_8$)] (**RuC$_8$-1**, acac = acetylacetonate, acacC$_8$ = 3-(4′-octyloxy-phenylalkynyl)-pentane-2,4-dionato), [Ru(acac)(acacC$_8$)$_2$] (**RuC$_8$-2**), [Ru(acacC$_8$)$_3$] (**RuC$_8$-3**), [Ru(acacC$_0$)$_3$] (**RuC$_0$-3**, acacC$_0$ = 3-(phenylalkynyl)-pentane-2,4-dionato), and [Ru(acacC$_{24}$)$_3$] (**RuC$_{24}$-3**, acacC$_{24}$ = 3-(3′,4′,5′-tri(octyloxy)-phenylalkynyl)-pentane-2,4-dionato). All the complexes, except for **RuC$_0$-3**, could be separated into Δ, Λ isomers by HPLC on a chiral column and were examined as chiral dopants for a nematic liquid crystal, *N*-(4-methoxybenzilidene)-4-butylaniline (MBBA). The Δ isomers of **RuC$_8$-1**, **RuC$_8$-2**, **RuC$_8$-3**, and **RuC$_{24}$-3** induced a right-handed (*P*) helix and the magnitudes of the HTPs (/μm^{-1}) were determined as follows: **RuC$_8$-1** (+60) < **RuC$_8$-2** (+109) > **RuC$_8$-3** (+78) > **RuC$_{24}$-3** (+41). The HTPs of the ruthenium dopants were not simply proportional to their size. The highest HTP observed in biaxial **RuC$_8$-2** was attributed to the balance of the molecular helicity and high ordering in MBBA based on the surface chirality model.

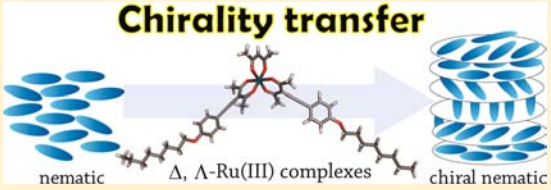

INTRODUCTION

Nematic liquid crystal (N) phases are known to transform into chiral nematic liquid crystal (N* or cholesteric liquid crystal) phases upon doping a small amount of chiral molecules (chiral dopants).[1,2] This threshold-less phenomenon has attracted much attention as a transfer and/or amplification of molecular chirality to a helical structure on a micrometer scale.[3−6] The extent of the chiral amplification, that is, the helical twisting power of a dopant (denoted by HTP or β_M), is represented by $\beta_M = 1/(x \cdot p)$, in which x is the molar fraction of a dopant and p is the pitch length of an induced helix. The positive and negative β_M values correspond to right-handed (*P*) and left-handed (*M*) helices, respectively. Several types of chiral dopants have been found to exhibit extremely high β_M values greater than 100 (/μm^{-1}).[7−11]

Theoretical approaches for understanding the mechanism of the transition from the N to N* phases have been also examined. In several cases, the molecular HTP has been theoretically reproduced with the aid of MD simulations.[12−15] However, the correlation between the molecular structure of a chiral dopant and induced helix is still implicit in many cases. The theoretical treatment of an organic dopant is often difficult because of the various conformations in liquid crystals. The magnitude of the β_M value, even its sign, is usually difficult to predict from the molecular structure of a dopant.

Δ- or Λ-tris-chelate metal complexes, in which three ligands are rigidly positioned in a propeller-like fashion, show several unique properties when used as chiral dopants.[16−19] Drake, Spada, et al. reported that Δ- or Λ-tris(acetyleacetonato) metal complexes, Δ, Λ-[M(acac)$_3$] (M = Cr, Co, Ru, Rh, Ir), exhibit high HTPs ($\beta_M = -102$ for Δ-[Ru(acac)$_3$]) in a nematic liquid crystal, *N*-(4-methoxybenzilidene)-4-butylaniline (MBBA).[16] In recent years, Yamagishi, Hoshino-Miyajima, and co-workers have examined the monosubstituted complex of the [Ru(acac)$_2$(L$_{backbone}$)] type as a chiral dopant, in which L$_{backbone}$ is an elongated β-diketonato ligand to align with liquid crystal molecules (Figure 1).[20−24] They have found that the handedness of an induced helix is determined by the direction of L$_{backbone}$.[22,24] That is, Δ-[Ru(acac)$_2$(L$_{backbone}$)] with the L$_{backbone}$ elongated perpendicular to the molecular C_2 axis (perpendicular type) induces the *M* helix, while Δ-[Ru(acac)$_2$(L$_{backbone}$)] with the L$_{backbone}$ elongated parallel to the C_2 axis (parallel type) induces the *P* helix (vice versa for the Λ isomer). The helical inversion driven by the direction of the L$_{backbone}$ has been theoretically interpreted by regarding that [Ru(acac)$_2$(L$_{backbone}$)] has one rigid conformation in liquid crystals. A rough calculation based on surface chirality model, which was developed by Ferrarini et al. and found to be a

Received: May 20, 2013
Published: September 13, 2013

   dx.doi.org/10.1021/ic401240f | *Inorg. Chem.* 2013, 52, 11042−11050

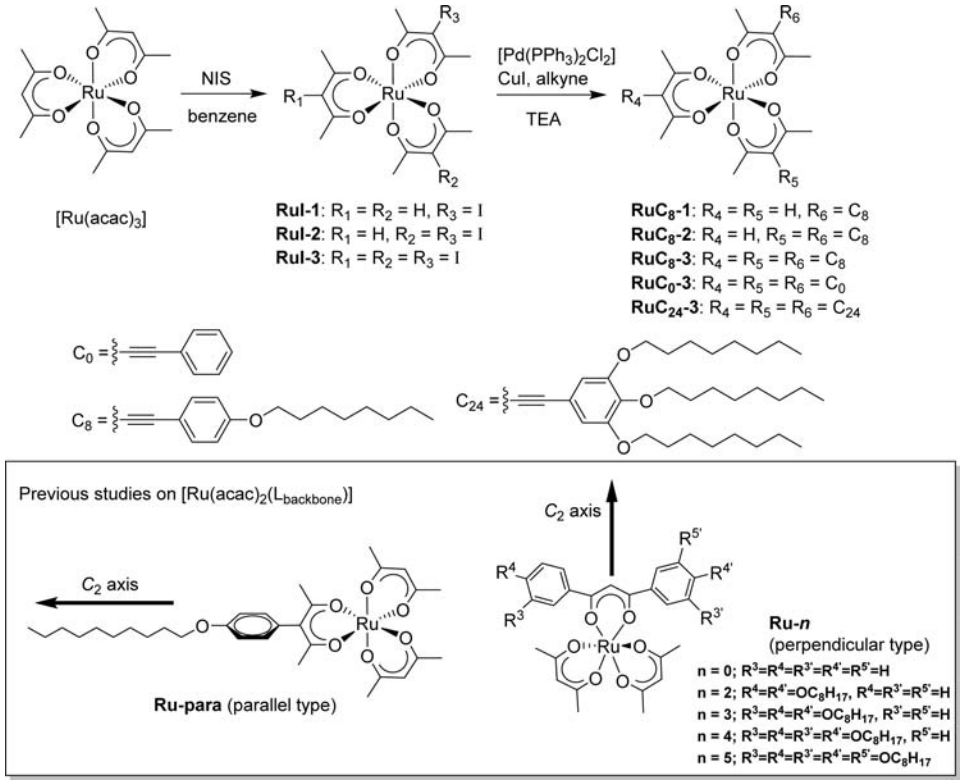

Figure 1. Ru(III) complexes (**RuC$_8$-1**, **RuC$_8$-2**, **RuC$_8$-3**, **RuC$_0$-3**, and **RuC$_{24}$-3**) discussed in the present paper and two types of complexes (**Ru-para** and **Ru-*n***) reported in a previous paper.[21,22]

powerful tool for interpreting dopant-host interactions,[25−30] has successfully confirmed that the sign of HTP is inverted depending on the direction of $L_{backbone}$.

The molecular structure-HTP correlation has been also investigated for $[Ru(acac)_2(L_{backbone})]$ type complexes (**Ru-*n***, Figure 1), in which a dibenzoylmethanate substituted with *n* octyloxy groups was used as $L_{backbone}$. As a result, uniaxial rod-like structure was concluded to be suitable for acquiring high HTP. The effect of one ligand ($L_{backbone}$) on the HTP has become clear to some extent, while those of the two remaining acac ligands in $[Ru(acac)_2(L_{backbone})]$ are still unclear. That is, structure-HTP correlation has not yet been confirmed for $[Ru(acac)(L_{backbone})_2]$ and $[Ru(L_{backbone})_3]$ types. Theoretically, the size of acac ligands in $[Ru(acac)_2(L_{backbone})]$ type is associated with the magnitude of the HTP.[22] Therefore, $[Ru(acac)(L_{backbone})_2]$ and $[Ru(L_{backbone})_3]$ have the possibility to show higher HTPs than $[Ru(acac)_2(L_{backbone})]$. However, the synthesis of the $[Ru(acac)(L_{backbone})_2]$ and $[Ru(L_{backbone})_3]$ types and their evaluation as chiral dopants have not been examined because of the difficult optical resolution of tris(*β*-diketonato) metal complexes with multiple bulky substituents such as alkyl chains.[31]

In the present paper, we systematically modified three acac ligands in $[Ru(acac)_3]$ to fully establish the molecular structure-HTP correlation; five new Ru(III) complexes, $[Ru(acac)_2(acacC_8)]$ (**RuC$_8$-1**, $acacC_8$ = 3-(4′-octyloxy-phenylalkynyl)-pentane-2,4-dionato), $[Ru(acac)(acacC_8)_2]$ (**RuC$_8$-2**), $[Ru(acacC_8)_3]$ (**RuC$_8$-3**), $[Ru(acacC_0)_3]$ (**RuC$_0$-3**, $acacC_0$ = 3-(phenylalkynyl)-pentane-2,4-dionato), and $[Ru(acacC_{24})_3]$ (**RuC$_{24}$-3**, $acacC_{24}$ = 3-(3′,4′,5′-tri(octyloxy)-phenylalkynyl)-pentane-2,4-dionato) were synthesized by the stepwise modification of $[Ru(acac)_3]$ (Figure 1). **RuC$_8$-1** has uniaxial rod-like structure, while others have biaxial, triaxial, or even disk-like structures. Moreover, we succeeded in the optical resolution of the complexes except for **RuC$_0$-3**. Further evaluation of the enantiomeric complexes as chiral dopants found that the HTPs ($/\mu m^{-1}$) of the Δ isomers are as follows: **RuC$_8$-1** (+60) < **RuC$_8$-2** (+109) > **RuC$_8$-3** (+78) > **RuC$_{24}$-3** (+41). The ruthenium complexes, especially biaxial **RuC$_8$-2**, showed relatively high HTPs compared to that of our previously reported compound, Δ-$[Ru(acac)_2(L_1)]$ (**Ru-para**, L_1 = 3-(4′-decyloxyphenyl)-pentane-2,4-dionato, β_M = 24). We will discuss the role of each *β*-diketonato ligand in the HTP.

EXPERIMENTAL SECTION

Physical Measurements. ^{1}H NMR spectra were recorded at 600 MHz with a Bruker AVANCE-II-600 or at 400 MHz with a Bruker AVANCE-III-400. All spectra are referenced to TMS. Mass spectrometry was performed with a ITQ-700 (Thermo Fisher Scientific) for EI-MS or with a Exactive Plus (Thermo Fisher Scientific) for ESI-MS; the mass range for high resolution ESI-MS was 20−2000 with a nominal resolution (at *m*/*z* 200) of 140.000. Elemental analyses were carried out with a Perkin-Elmer 2400II. UV−vis and circular dichroism (CD) spectra were recorded with JASCO V-570 and J-720 spectrometers. The CD spectra of liquid crystal materials doped with enantiomeric Ru(III) complexes were measured using a homogeneous alignment cell of 10 μm thickness (RP type, EHC, Japan). HTP measurements were performed by the Cano method using a wedge cell (EHC, Japan)[32] and controlling the temperature at 30 ± 0.1 °C by a self-made hot stage with a temperature control unit (E5CN, OMRON Inc.).

Materials. *N*-(4-methoxybenzylidene)-4-butylaniline was purchased from TCI (Japan) and used without further purification. $[Ru(acacI)_3]$ was prepared according to a literature procedure.[33] 3′,4′,5′-tri(octyloxy)phenylacetylene were prepared according to a literature procedure,[34] while 4′-octyloxyphenylacetylene was newly synthesized by modifying the reported procedure. Sonogashira−Hagihara reaction was performed by reference to a previous paper.[35]

dx.doi.org/10.1021/ic401240f | Inorg. Chem. 2013, 52, 11042−11050

4′-Octyloxyphenylacetylene (C_8). A pale yellow oil. ^{1}H NMR (400 MHz, $CDCl_3$, δ): 7.41 (d, J = 9.2 Hz, 2H), 6.82 (d, J = 9.2 Hz, 2H), 3.94 (t, J = 6.6 Hz, 2H), 2.98 (s, 1H), 1.77 (quint, J = 7.1 Hz, 2H), 1.41−1.48 (m, 2H), 1.27−1.35 (m, 8H), 0.89 (t, J = 6.6 Hz, 3H). EI-MS: m/z 230.0 ([M]$^+$).

Synthesis of [Ru(acac)$_2$(acacI)] and [Ru(acac)(acacI)$_2$]. To benzene (50 mL), [Ru(acac)$_3$] (3.51 g, 8.8 mmol) and *N*-iodosuccinimide (2.97 g, 13.2 mmol) were added, and the mixture was refluxed for 20 min. The reaction was monitored by TLC (benzene/acetonitrile = 10/1, v/v). The solvent was removed by rotary-evaporator and the residue was subjected to silica gel column chromatography with benzene/acetonitrile = 15/1 (v/v) as an eluent. From the first and second bands, [Ru(acac)(acacI)$_2$] and [Ru(acac)$_2$(acacI)] were isolated as a violet solid (2.10 g, 45%) and a dark red solid (1.75 g, 31%), respectively.

[Ru(acac)$_2$(acacI)]. Anal. Calcd (%) for $C_{15}H_{20}IO_6Ru$: C 34.36; H 3.84. Found: C 34.43; H 3.99. ^{1}H NMR (400 MHz, $CDCl_3$, δ): −5.09 (s, 6H), −5.44 (s, 6H), −7.41 (s, 6H), −33.45 (s, 2H). HRMS (ESI$^+$): calculated for $C_{15}H_{21}IO_6Ru$ ([**RuI-1**+H]$^+$) 525.9421, found 525.9425.

[Ru(acac)(acacI)$_2$]. Anal. Calcd (%) for $C_{15}H_{19}I_2O_6Ru$: C 27.71, H 2.95; found: C 28.07, H 2.98. ^{1}H NMR (600 MHz, C_6D_6, δ): −3.47 (s, 6H), −6.50 (s, 6H), −9.08 (s, 6H), −37.68 (s, 1H). HRMS (ESI$^+$): calculated for $C_{15}H_{20}I_2O_6Ru$ ([**RuI-2**+H]$^+$) 651.8387, found 651.8388.

Synthesis of [Ru(acac)$_2$(acacC_8)] (RuC_8-1). To the triethylamine (60 mL), [Ru(acac)$_2$(acacI)] (0.735 g, 1.13 mmol), (4′-octyloxyphenyl)acetylene (0.35 g, 1.52 mmol), [PdCl$_2$(PPh$_3$)$_2$] (20 mg, 0.028 mmol), and CuI (11 mg, 0.058 mmol) were added. Then, the mixture was stirred at ambient temperature under a nitrogen atmosphere. On the second and third days, additional 4′-octyloxyphenylacetylene (0.35 g, 1.52 mmol), [PdCl$_2$(PPh$_3$)$_2$] (20 mg, 0.028 mmol), and CuI (15 mg, 0.079 mmol) were added. After stirring for a total of three days, the solvent was removed by evaporation, and the residue was subjected to silica gel column chromatography with benzene as an eluent. From the first eluted band, [Ru(acac)$_2$(acacC_8)] was isolated as a violet solid (0.306 g, 51% yield). Anal. Calcd (%) for $C_{31}H_{41}O_7Ru$: C 59.41, H 6.59; found: C 59.23, H 6.55. ^{1}H NMR (600 MHz, $CDCl_3$, δ): 7.73 (d, J = 9.0 Hz, 2H), 4.39 (d, J = 9.0 Hz, 2H), 4.23 (t, J = 6.6 Hz, 2H), 1.68 (quint, J = 7.2 Hz, 2H), 1.39 (quint, J = 7.4 Hz, 2H), 1.21−1.32 (m, 8H), 0.86 (t, J = 7.2 Hz, 3H), −4.08 (s, 6H), −5.99 (s, 6H), −7.26 (s, 6H), −33.60 (s, 2H). HRMS (ESI$^+$): calculated for $C_{32}H_{41}O_7Ru$ ([**RuC$_8$-1**+H]$^+$) 628.1969, found 628.1971.

Synthesis of [Ru(acac)(acacC_8)$_2$] (RuC_8-2) and [Ru(acacC_8)$_3$] (RuC_8-3). These complexes were synthesized according to a similar procedure to that of **RuC$_8$-1** by using [Ru(acac)(acacI)$_2$] and [Ru(acacI)$_3$] instead of [Ru(acac)$_2$(acacI)], respectively.

RuC$_8$-2: a green solid, 44% yield. Anal. Calcd (%) for $C_{47}H_{61}O_8Ru$: C 66.02, H 7.19; found: C 66.55, H 7.48. ^{1}H NMR (400 MHz, $CDCl_3$, δ): 7.79 (d, J = 8.0 Hz, 4H), 4.26 (t, J = 6.4 Hz, 4H), 4.19 (d, J = 8.0 Hz, 4H), 1.67 (quint, J = 7.0 Hz, 4H), 1.37−1.41 (m, 4H), 1.25−1.30 (m, 16H), 0.86 (t, J = 6.0 Hz, 6H), −4.42 (s, 6H), −5.97 (s, 6H), −7.67 (s, 6H), −36.06 (s, 1H). HRMS (ESI$^+$): calculated for $C_{47}H_{62}O_8Ru$ ([**RuC$_8$-2**+H]$^+$) 856.3483, found 856.3479.

RuC$_8$-3: a green pasty solid, 13% yield. Anal. Calcd (%) for $C_{63}H_{81}O_9Ru$: C 69.84, H 7.54; found: C 69.37, H 7.83. ^{1}H NMR (400 MHz, $CDCl_3$, δ): 7.85 (d, J = 8.4 Hz, 6H), 4.29 (t, J = 6.6 Hz, 6H), 3.93 (d, J = 8.4 Hz, 6H), 1.66 (quint, J = 7.5 Hz, 6H), 1.38 (quint, J = 7.5 Hz, 6H), 1.22−1.29 (m, 24H), 0.85 (t, J = 6.9 Hz, 9H), −6.55 (s, 18H). HRMS (ESI$^+$): calculated for $C_{63}H_{81}O_9Ru$ ([**RuC$_8$-3**+H]$^+$) 1084.4997, found 1084.5018.

Synthesis of [Ru(acacC_0)$_3$] (RuC_0-3). To the triethylamine (140 mL), [Ru(acacI)$_3$] (1.91 g, 2.46 mmol) was added and stirred at ambient temperature under a nitrogen atmosphere. Then, phenylacetylene (1.6 mL, 14.6 mmol), [PdCl$_2$(PPh$_3$)$_2$] (78 mg, 0.11 mol), and CuI (26 mg, 0.14 mmol) were added. After 3 h, additional phenylacetylene (0.40 mL, 7.28 mmol), [PdCl$_2$(PPh$_3$)$_2$] (74 mg, 0.11 mmol), and CuI (30 mg, 0.16 mmol) were added, and the solution was stirred overnight. The solvent was removed by evaporation, and the residue was subjected to silica gel column chromatography with benzene/hexane = 3/2 (v/v) as an eluent. From the first eluted band, [Ru(acacC_0)$_3$] was isolated as a green solid (0.216 g, 13% yield). Anal. Calcd (%) for $C_{39}H_{33}O_6Ru$: C 67.04, H 4.76; found: C 66.70, H 4.85. ^{1}H NMR (400 MHz, $CDCl_3$, δ): 8.50 (t, J = 8.0 Hz, 6H), 3.88 (d, J = 7.6 Hz, 3H), 3.81 (t, J = 7.6 Hz, 6H), −6.20 (s, 18H). HRMS (ESI$^+$): calculated for $C_{39}H_{34}O_6Ru$ ([**RuC$_0$-3**+H]$^+$) 700.1393, found 700.1403.

Synthesis of [Ru(acacC_{24})$_3$] (RuC_{24}-3). To the triethylamine (60 mL), [Ru(acacI)$_3$] (0.76 g, 0.97 mmol) was added and stirred at ambient temperature under a nitrogen atmosphere. Then, 3′,4′,5′-tri(octyloxy)phenylacetylene (2.91 g 6.0 mmol), [PdCl$_2$(PPh$_3$)$_2$] (90 mg, 0.13 mmol), and CuI (50 mg, 0.26 mmol) were added in four aliquots over 3 days. After stirring for a total of 3 days, the solvent was removed by evaporation, and the residue was subjected to silica gel column chromatography with dichloromethane/hexane = 6/1 (v/v) as an eluent. From the first eluted band, [Ru(acacC_{24})$_3$] was isolated as a green pasty solid (0.21 g, 12% yield). Anal. Calcd (%) for $C_{111}H_{177}O_{15}Ru$: C 71.96, H 9.63; found: C 72.11, H 10.03. ^{1}H NMR (400 MHz, $CDCl_3$, δ): 3.79 (t, J = 6.4 Hz, 12H), 3.74 (t, J = 6.4 Hz, 6H), 3.32 (s, 6H), 1.62−1.74 (m, 18H), 1.25−1.39 (m, 90H), 0.83−0.88 (m, J = 5.8 Hz, 27H), −6.37 (s, 18H). HRMS (ESI$^+$): calculated for $C_{111}H_{177}O_{15}Ru$ ([**RuC$_{24}$-3**]$^+$) 1853.2159, found 1853.2237.

Enantioselective Liquid Chromatography. Optical resolution of the ruthenium complexes was performed by high performance liquid chromatography (HPLC) on a JAI Co., Ltd. LC-9204 system with a chiral column. Enantioseparations of all complexes (**RuC$_8$-1**, **RuC$_8$-2**, **RuC$_8$-3**, **RuC$_0$-3**, and **RuC$_{24}$-3**) were examined on chiral stationary phase (CSP) based on 3,5-dimethylphenylcarbamate of amylose (Chiralpak IA, Daicel Chemical Industries, Ltd., Tokyo, Japan). As a mobile phase, *n*-hexane/2-propanol (20/1−24/1, v/v) or *n*-hexane/chloroform (20/1, v/v) was used. Enantioseparation of **RuC$_8$-1** was also performed on a column packed with an ion-exchanged material of synthetic hectorite and Δ-[Ru(phen)$_3$]$^{2+}$ (Ceramosphere RU-1, Shiseido, Japan) with methanol/chloroform = 99/1 (v/v) as a mobile phase. Chromatograms of each complex are shown in the Supporting Information.

Crystal Structure Determination. The crystal structures of [Ru(acac)$_2$(acacI)], [Ru(acac)(acacI)$_2$], [Ru(acacI)$_3$], [Ru(acac)$_2$(acacC_8)] (**RuC$_8$-1**), and [Ru(acacC_0)$_3$] (**RuC$_0$-3**) were determined by the single-crystal X-ray diffraction method. In the case of **RuC$_0$-3**, the analysis was performed for the chiral crystal composed of ΔΔ-**RuC$_0$-3** because extensive disordering of alkyl chains were found for the racemic crystal of **RuC$_0$-3**. For the collection of the diffraction data, a Bruker APEX II ULTRA diffractometer was used. The structures were solved by the direct method using the program SHELXS-97.[36] The refinement and all further calculations were carried out using the program SHELXL-97.[36] All non-H atoms were refined anisotropically, using weighted full-matrix least-squares on F^2. In **RuI-2**, solvent accessible voids of 309 Å^3 still remain in the crystal structure. In this space, solvent molecules were assumed to exist, while they could not be determined by X-ray study and elemental analysis because of severe positional disorder and/or gradual liberation at room temperature. Refinement was done by Platon/Squeeze[37] to account for these species. Crystallographic and experimental data are summarized in Supporting Information, Table S1.

Computational Method. All ab initio molecular orbital (MO) calculations were carried out using the Gaussian 03 program.[38] The geometries of model compounds, [Ru(acac)$_2$(acacPh)] (acacPh = 3-phenyl-pentane-2,4-dionato) and [Ru(acac)$_2$(acacC_2Ph)] (acacC_2Ph = 3-phenylalkynyl-pentane-2,4-dionato) were optimized at the unrestricted B3LYP level, using the LANL2DZ basis set with the associated effective core potential (ECP) for Ru and 6-311G(d, p) basis sets for the other atoms as implemented in the Gaussian 03 program. The optimized structure was found to be a minimum by frequency calculations.

RESULTS AND DISCUSSION

Synthesis and Optical Resolution. To clarify the structure-HTP relations in Δ, Λ chiral dopants, we designed five new Ru(III) complexes (**RuC$_8$-1**, **RuC$_8$-2**, **RuC$_8$-3**, **RuC$_0$-**

3, and **RuC$_{24}$-3**) by changing their structures in stepwise fashion from rod to disk. **RuC$_8$-1** has a uniaxial rod structure, similarly with the previously reported compound **Ru-para**, while **RuC$_8$-2** and **RuC$_8$-3** have multiple ligands elongated parallel to the C_2 axis. **RuC$_8$-2** and **RuC$_8$-3** have bi- and triaxial structures, respectively.[39] Moreover, we also designed disk-like complexes, **RuC$_0$-3** and **RuC$_{24}$-3**. The overall synthetic procedure is outlined in Figure 1.

It was already reported that the treatment of [Ru(acac)$_3$] with 9 equiv of *N*-iodosuccinimide (NIS) at a reflux condition afforded [Ru(acacI)$_3$] (**RuI-3**, acacI = 3-iodo-pentane-2,4-dionato).[34] We examined the reaction of [Ru(acac)$_3$] with 1.5 equiv of NIS to obtain a mixture of [Ru(acac)$_2$(acacI)] (**RuI-1**) and [Ru(acac)(acacI)$_2$] (**RuI-2**) (see details in Experimental Section). The mixture was separated and purified by silica gel column chromatography. The structure of each complex was finally determined by single crystal X-ray diffraction. The palladium-catalyzed alkynylations of **RuI-1**, **RuI-2**, and **RuI-3** with 4′-octyloxyphenylacetylene under Sonogashira–Hagihara conditions afforded [Ru(acac)$_2$(acacC$_8$)] (**RuC$_8$-1**, acacC$_8$ = 3-(4′-octyloxy-phenylalkynyl)-pentane-2,4-dionato), [Ru(acac)-(acacC$_8$)$_2$] (**RuC$_8$-2**), and [Ru(acacC$_8$)$_3$] (**RuC$_8$-3**) in 51%, 44%, and 13% yields, respectively. Moreover, [Ru(acacC$_0$)$_3$] (**RuC$_0$-3**, acacC$_0$ = 3-(phenylalkynyl)-pentane-2,4-dionato) and [Ru(acacC$_{24}$)$_3$] (**RuC$_{24}$-3**, acacC$_{24}$ = 3-(3′,4′,5′-tri(octyloxy)-phenylalkynyl)-pentane-2,4-dionato) were obtained by Sonogashira coupling of **RuI-3** with phenylacetylene and 3′,4′,5′-tri(octyloxy)phenylacetylene in 13% and 12% yields, respectively.

We then examined the optical resolution of the five Ru(III) complexes by HPLC on a chiral column that has a bonded amylose based chiral stationary phase (Chiralpak IA, Daicel Chemical Industries, Ltd., Japan). For **RuC$_8$-2**, **RuC$_8$-3**, and **RuC$_{24}$-3**, two well-separated major peaks were observed to the baseline separation in the chromatograms using hexane/2-propanol = 96/4 or 20/1 (v/v) as the solvent (Supporting Information, Figure S8). In contrast, **RuC$_8$-1** was only partially resolved under the same conditions. The optical resolution of **RuC$_0$-3** was examined using hexane/chloroform = 20/1 (v/v) as the solvent because of its low solubility in hexane/2-propanol, but it could not be resolved at all. For the optical resolution with CHIRALPAK IA, an octyloxy group improved the efficiency of the optical resolution as found in the extremely good separation of **RuC$_{24}$-3** with nine octyloxy groups. The octyloxy groups probably enhanced the interaction between the ruthenium complexes and the surface of the column. The optical resolution of **RuC$_8$-1** was finally accomplished by a clay column fied with Δ-[Ru(phen)$_3$]$^{2+}$ (Ceramospher RU1, SHISEIDO, Japan), which has been effective for the optical resolution of various tris(*β*-diketonato) Ru(III) complexes with relatively simple structures.[40]

UV–vis and CD Measurements. Figure 2 shows the UV–vis spectra of **RuC$_8$-1**, **RuC$_8$-2**, **RuC$_8$-3**, and **RuC$_{24}$-3** measured in chloroform. All the complexes showed three absorption bands at about 300, 350, and 500–700 nm. [Ru(acac)$_3$] is reported to show mainly three absorptions with peaks at 272, 349, and 506 nm in an acetonitrile solution. The dominant character of each absorption is attributed to $\pi-\pi^*$ (triplet), LMCT, and $\pi-\pi^*$ (singlet) transitions, respectively.[41] The three absorption bands commonly observed in **RuC$_8$-1**, **RuC$_8$-2**, **RuC$_8$-3**, and **RuC$_{24}$-3** can be assigned as in the case of [Ru(acac)$_3$]. The molar absorption coefficients (ε) of the complexes increased in the order of **RuC$_8$-1** < **RuC$_8$-2** < **RuC$_8$-3** ≈ **RuC$_{24}$-3** for each absorption band, accompanied by a slight red-shift in the peaks. Molar absorption of the complexes increased as the number of phenylalkyne moieties increased.

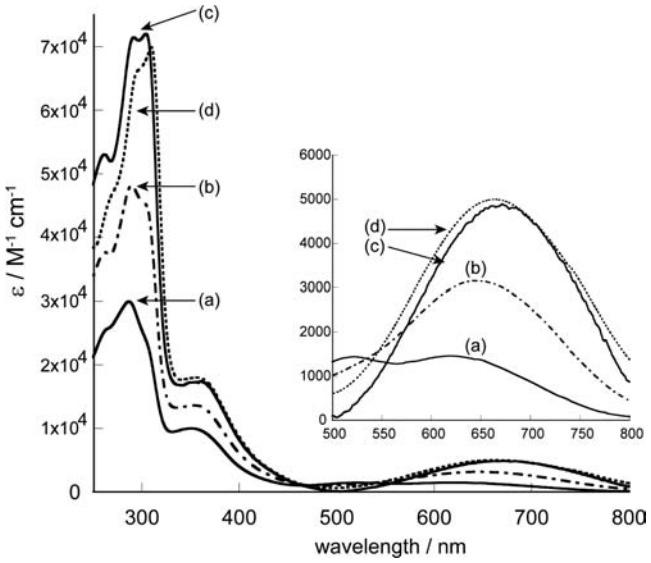

Figure 2. UV–vis spectra of (a) **RuC$_8$-1**, (b) **RuC$_8$-2**, (c) **RuC$_8$-3**, and (d) **RuC$_{24}$-3** measured in chloroform. Inset shows the enlarged view of the range from 500 to 800 nm.

Figure 3 shows the CD spectra of the less- and more-retained fractions of **RuC$_8$-1**, **RuC$_8$-2**, **RuC$_8$-3**, and **RuC$_{24}$-3** divided by the chiral HPLC. The measurements were done in chloroform solution. The spectra of the two fractions in each complex are mirror images of one another. The assignment of the Δ or Λ configuration was possible by comparing the CD spectra to that of Δ- and Λ-[Ru(acac)$_3$].[41] Δ-[Ru(acac)$_3$] shows the positive and negative Cotton effects at about 415 and 350 nm, respectively. In the case of **RuC$_8$-1** resolved by the clay column, the Δ and Λ isomers were isolated from the more- and less-retained fractions. For **RuC$_8$-2** and **RuC$_8$-3** resolved by the CHIRALPAK IA column, the less- and more-retained fractions were assigned to the Δ and Λ isomers, respectively. Notably,

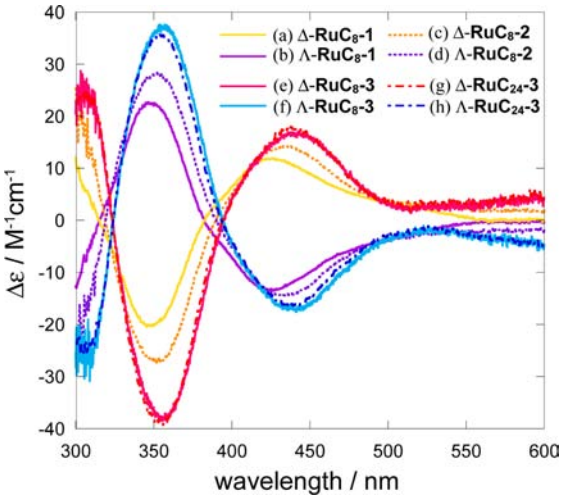

Figure 3. CD spectra of (a, b) **RuC$_8$-1**, (c, d) **RuC$_8$-2**, (e, f) **RuC$_8$-3**, and (g, h) **RuC$_{24}$-3**, measured in chloroform. The spectra of (b), (c), (e), and (h) correspond to the less-retained fractions, while the spectra of (a), (d), (f), and (g) correspond to the more-retained fractions.

dx.doi.org/10.1021/ic401240f | *Inorg. Chem.* 2013, 52, 11042–11050

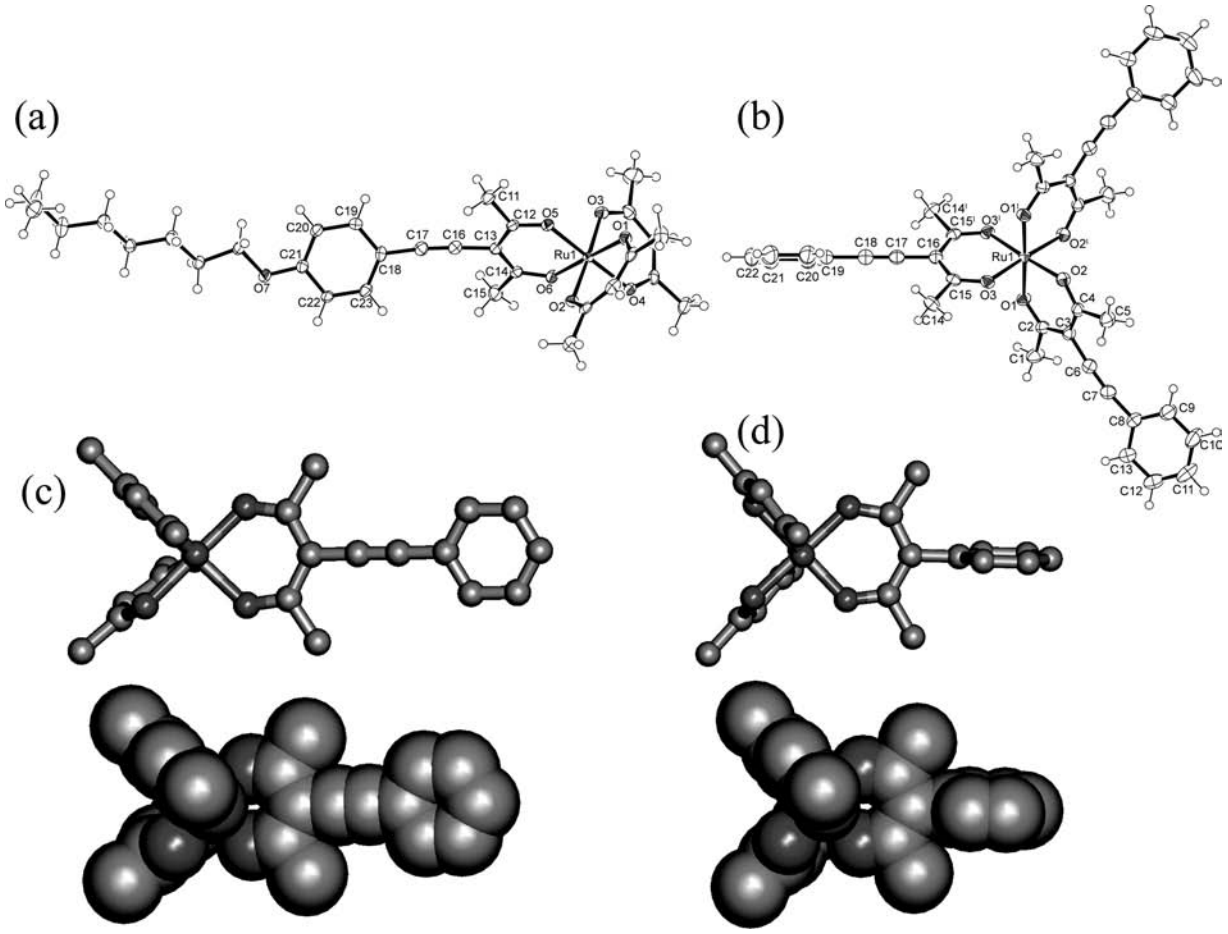

Figure 4. ORTEP representations of the molecular structure of (a) Δ-**RuC$_8$-1**, and (b) **RuC$_0$-3**. (50% probability level, symmetry code; I: $-x$, y, $-z$ +3/2). Molecular structures of (c) [Ru(acac)$_2$(acacC$_2$Ph)] (acacC$_2$Ph = 3-phenylalkynyl-pentane-2,4-dionato) and (d) [Ru(acac)$_2$(acacPh)] (acacPh = 3-phenyl-pentane-2,4-dione) optimized at the UB3LYP/(LanL2DZ+6-311G**) level and drawn using ball-stick and space-filling models.

the order of elution is reversed in the case of **RuC$_{24}$-3** in spite of the use of the same column (CHIRALPAK IA); the Δ and Λ isomers were isolated from the more-and less-retained fractions, respectively. A specific interaction between the octyloxy group and the column surface is interesting in the sense that simple alkoxy groups may widely enhance the efficiency of the optical resolution, while a further investigation was not performed in this study. The racemization of every complex was not observed at least at ambient temperature.

Crystal and Optimized Structures. Of the five target complexes (**RuC$_8$-1** ∼ **RuC$_{24}$-3**), single crystals suitable for single crystal X-ray diffraction studies were obtained for **RuC$_8$-1** and **RuC$_0$-3**. For **RuC$_8$-1**, both the racemic and enantiomeric complexes formed single crystals. Severe disorders of alkyl chains were observed for the former crystal, while an ordered structure was observed for the latter. Therefore, structural refinement was completed for the crystal composed of the Δ isomers. The detailed crystallographic data of **RuC$_8$-1** and **RuC$_0$-3**, in addition to **RuI-1**, **RuI-2**, and **RuI-3** used as intermediates, are shown in the Supporting Information, Table S1.

In the crystal structures of **RuC$_8$-1** and **RuC$_0$-3**, the C$_8$ and phenylalkyne units are elongated parallel to the C_2 axis, respectively (Figure 4). The C≡C distances found in **RuC$_8$-1** and **RuC$_0$-3** (1.160(6)-1.203(4) Å) are typical values of a carbon−carbon triple bond. In both complexes, the phenylene moieties are tilted toward the acac planes. The dihedral angles between the two moieties in **RuC$_8$-1** and **RuC$_0$-3** are in the range from 32.6 to 46.3°, while a specific steric interaction between the moieties is not observed. The phenylene units may rotate toward the acac unit to some extent in the solution and liquid crystals. In the case of **Ru-para**, the phenylene group is directly linked to the 3-position of the acac without an alkyne spacer. Bulky groups introduced at the 3-position of the acac ligands are often stabilized at the almost orthogonal position because of the steric hindrance by the methyl groups.[42]

We further performed the density functional theory (DFT) calculations for the model compounds, [Ru(acac)$_2$(acacPh)] (acacPh = 3-phenyl-pentane-2,4-dionato) and [Ru(acac)$_2$(acacC$_2$Ph)] ((acacPh = 3-phenylalkynyl-pentane-2,4-dionato)), to clarify the role of the alkyne spacer in the acacC$_8$ ligand. The complexes could be regarded as the simplified structure of **Ru-para** and **RuC$_8$-1** without terminal alkoxy chains, respectively. The energy-minimized structures of [Ru(acac)$_2$(acacPh)] and [Ru(acac)$_2$(acacC$_2$Ph)] are shown in Figure 4, and they support the planarity of the acacC$_8$ ligand. The dihedral angle between the acac and phenylene moieties in the optimized structure of [Ru(acac)$_2$(acacC$_2$Ph)] is 7.5°. In contrast, the phenyl group is almost orthogonal to the acac with the dihedral angle of 87.4° in [Ru(acac)$_2$(acacPh)]. **RuC$_8$-1** has a structure similar to **Ru-para** at first glance. However, they have a different stereochemistry because of the presence or absence of an alkyne linker. The effect of the dopant structure on the HTP is discussed in a subsequent section.

dx.doi.org/10.1021/ic401240f | *Inorg. Chem.* 2013, 52, 11042−11050

HTP Measurements. The enantiomers of **RuC$_8$-1**, **RuC$_8$-2**, **RuC$_8$-3**, and **RuC$_{24}$-3** were dissolved in a room-temperature liquid crystal, *N*-(4-methoxybenzilidene)-4-butylaniline (MBBA). **RuC$_8$-1**, **RuC$_8$-3**, and **RuC$_{24}$-3** showed good solubility at least up to 0.35 mol %. In contrast, microcrystals were observed to be separated during the microscope observations when more than 0.20 mol % **RuC$_8$-2** was doped into MBBA. A molecular HTP (β_M; eq 1) was evaluated by the Cano method as described in the Experimental Section. The inverse of the pitch length (p^{-1}) was plotted versus the molar fraction (x) of the dopant (Figure 5). The slopes of the fitted

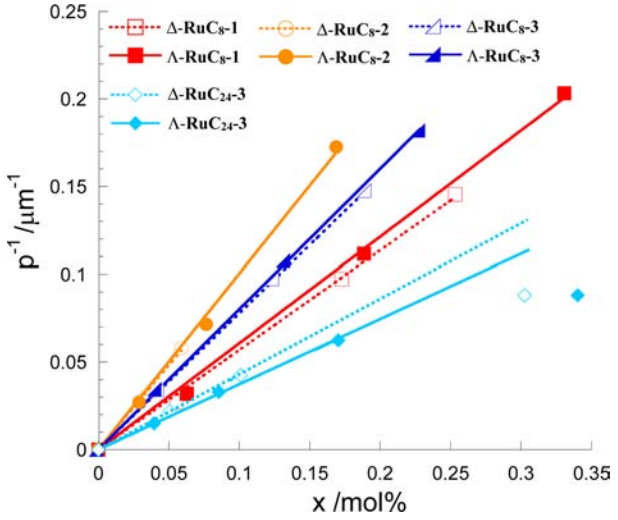

Figure 5. Plots of the inverse of helical pitch (p^{-1}) versus the molar fraction (x) of **RuC$_8$-1** (drawn in red), **RuC$_8$-2** (orange), **RuC$_8$-3** (blue), and **RuC$_{24}$-3** (cyan) doped in MBBA.

lines correspond to the magnitude of HTP. A linear correlation was observed for the cases of **RuC$_8$-1**, **RuC$_8$-2**, and **RuC$_8$-3**, while the points at the higher concentrations deviate from the linear correlation in the case of **RuC$_{24}$-3**. A specific dopant–dopant interaction is indicated for **RuC$_{24}$-3** at the higher concentrations. The HTP of **RuC$_{24}$-3** was determined from the points at the concentrations less than 0.20 mol %. The sign of HTP was determined by measuring the CD spectra of the MBBA samples doped with the Δ or Λ complexes. Helical arrangements of the host molecules in a chiral nematic phase exhibit a strong signal in the CD spectrum (induced CD, ICD).[42,43] Figure 6 shows the CD spectra of MBBA doped with the Δ, Λ isomers of **RuC$_8$-1**, **RuC$_8$-2**, **RuC$_8$-3**, and **RuC$_{24}$-3** . Every sample showed a strong band around 420 nm (ICD), attributed to the helical arrangement of the host molecules in a chiral nematic phase. The positive or negative ICD was related to the formation of the *P* (right-handed) or *M* (left-handed) helix, respectively.[43,44] The results of the HTP measurements are summarized in Table 1.

Δ-[Ru(acac)$_3$] is known to induce a left-handed (*M*) helix, while the Δ isomers of **RuC$_8$-1**, **RuC$_8$-2**, **RuC$_8$-3**, and **RuC$_{24}$-3** induced right-handed (*P*) helices (vice versa for the Λ isomers). These results reconfirmed that the introduced functional groups aligned parallel to the molecular C_2 axis induce an opposite-handed helix to that of the [Ru(acac)$_3$] core, as previously established for the uniaxial [Ru(acac)$_2$(L$_{backbone}$)] type.[24] In contrast, the magnitude of HTP was not simply proportional to the dopant size.

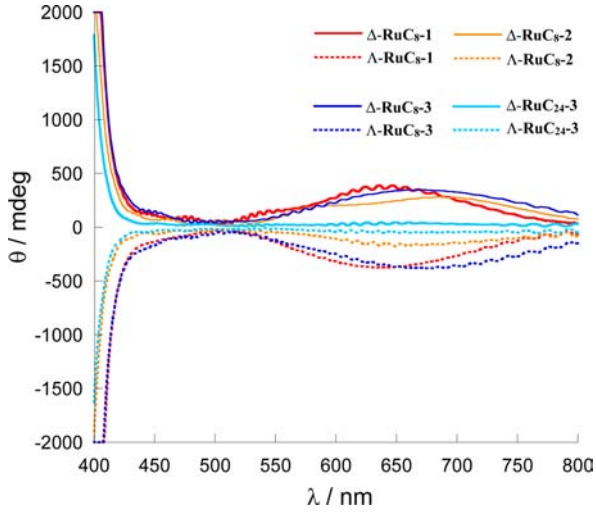

Figure 6. Induced circular dichroism spectra of MBBA samples doped with Δ, Λ-**RuC$_8$-1** (drawn in red), Δ, Λ-**RuC$_8$-2** (orange), Δ, Λ-**RuC$_8$-3** (blue), and Δ, Λ-**RuC$_{24}$-3** (cyan). The samples doped with the Δ and Λ isomers are drawn with solid and dotted lines, respectively. A monitoring light was incident in the normal direction or along the helical axis.

The HTP of **RuC$_8$-1** was more than two times that of **Ru-para**, although they have similar structures. The different structural parts between the complexes are an alkyne spacer and alkyl length (C10 for **Ru-para** and C8 for **RuC$_8$-1**). We consider that the former factor is the main reason of their different HTP values, because replacement of the decyloxyphenylene unit in **Ru-para** to the azobenzene moiety with a butoxy chain resulted in a slight increase of HTP (32 for Δ isomer) in a previous study.[24] The phenylene moiety in **RuC$_8$-1** can rotate toward acac to some extent as indicated from the crystal structures and DFT optimized structures, while the two units are stabilized at the almost orthogonal position in **Ru-para**. The microscopic interaction between the Ru complex and surrounding liquid crystal molecules is the source of the helical induction. Although a detailed description of the actual interaction has not yet been established, we consider that the planar ligand structure in **RuC$_8$-1** enhances the association with the MBBA molecules and the efficiency of the chiral transfer, resulting in a higher HTP.

In contrast, the biaxial and triaxial complexes, **RuC$_8$-2** and **RuC$_8$-3**, showed higher HTPs than **RuC$_8$-1**. The result is different from the case of **Ru-*n***, in which biaxial complexes showed lower HTPs than the uniaxial complex.[21] We now deduce the result of a theoretical calculation based on a surface chirality model to interpret the different HTPs among the Ru(III) complexes.[25−30] The surface chirality model developed by Ferrarini et al. accounts for the microscopic dopant-liquid crystal interactions based on the molecular surface. The theory has been applied to various chiral dopants, including the Δ, Λ-metal complexes of the [Ru(acac)$_2$(L$_{backbone}$)] type.[21,22] Based on this theory, HTP (β_M) is expressed by the following equation

$$\beta_M = \left(\frac{RT\xi}{2\pi K_{22}\upsilon_m}\right)Q \qquad (1)$$

where R is the gas constant, T is the temperature, K_{22} is the twist elastic constant, ξ is the interaction energy, and υ_m is the molar volume of the solution. By using an ordering matrix (S_{ij})

dx.doi.org/10.1021/ic401240f | Inorg. Chem. 2013, 52, 11042−11050

Table 1. Values for HTP ($\beta_M/\mu m^{-1}$) of Δ-, Λ-RuC_8-1, RuC_8-2, RuC_8-3, RuC_{24}-3, Ru-para, and [Ru(acac)$_3$] in MBBA (30 °C)

chirality	RuC_8-1	RuC_8-2	RuC_8-3	RuC_{24}-3	Ru-para[a]	[Ru(acac)$_3$][a]
Δ isomer	60	109	78	41	24	−102
Λ isomer	−64	−107	−80	−36	−25	not determined

[a]Cited from previous reports.[16,22]

and helicity tensor Q_{ij} based on a molecular helix, **Q** is expressed by the following equations

$$\mathbf{Q} = -\sqrt{\frac{2}{3}}\,(Q_{xx}S_{xx} + Q_{yy}S_{yy} + Q_{zz}S_{zz}) \tag{2}$$

$$Q_{ij} = \sqrt{\frac{3}{8}}\int_S [S_i(\hat{s}\times\vec{r})_j + (\hat{s}\times\vec{r})_i S_j]\,d\vec{r} \tag{3}$$

Here, we have calculated the helicity tensor Q_{ii} for the model of Δ-RuC_8-3. As shown in Figure 7, the model is composed of six

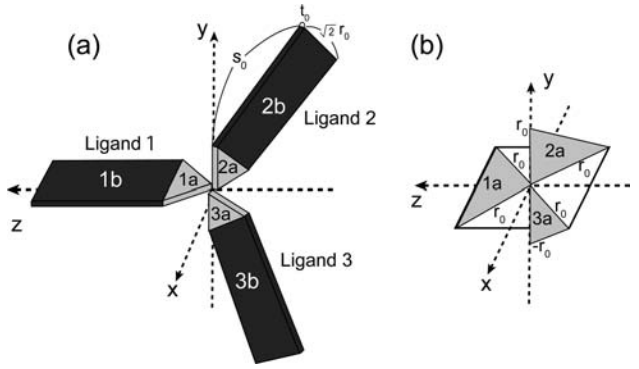

Figure 7. (a) Structural model of Δ-RuC_8-3 for the calculation based on surface chirality model. The z axis was taken to be parallel to the ligand 1. The 1a, 2a, and 3a parts are thin triangular prisms, in which the basal planes are isosceles right triangles with legs of length r_0. The 1b, 2b, and 3b parts are thin rectangular cuboids with dimensions of $\sqrt{2}r_0 \times S_0 \times t_0$. (b) Enlarged view of the central parts (1a, 2a, 3a), corresponding to [Ru(acac)$_3$] core.

parts (1a, 1b, 2a, 2b, 3a, 3b), and its one ligand (ligand 1) was taken to be parallel to the z axis. The 1a, 2a, and 3a parts, corresponding to acac ligands, are thin triangular prisms, in which the basal planes are isosceles right triangles with legs of length r_0. The 1b, 2b, and 3b parts, corresponding to the C_8 group, are thin rectangular cuboids, in which the dimensions are $\sqrt{2}r_0$, s_0, and $t_0 \approx 0$. The effect of side faces in the six parts is negligible in the calculation of Q_{ij}. The details of the calculation are shown in Supporting Information. As a result, the three components of the helicity tensor (Q_{xx}, Q_{yy}, Q_{zz}) are derived as the sum of the contribution from six parts as shown in eq 4 where first and second terms in Q_{xx} and Q_{zz} are the contribution from the 2b and 3b units, respectively, and the third term is the contribution from the 1a, 2a, and 3a parts ([Ru(acac)$_3$] unit). The 1b part only determines the ordering direction and has no effect for the helicity tensor. In the case of RuC_8-2 type, the first or second member in Q_{xx} and Q_{zz} is 0 (s_0 = 0), while both first and second members are 0 in the case of RuC_8-1 type. According to the calculation, the absolute value of Q_{xx} and Q_{zz} for the ruthenium dopants are in the following order: RuC_8-1 < RuC_8-2 < RuC_8-3 ≈ RuC_{24}-3. Therefore, when dopants are aligned to the local director of the nematic host (S_{zz} has larger value than S_{xx} and S_{yy} under the condition of $S_{xx} + S_{yy} + S_{zz} = 0$), absolute values of **Q** and β_M calculated

$$\begin{cases} Q_{xx} = \dfrac{\sqrt{3}}{2}\left(r_0^2 s_0 + \dfrac{1}{\sqrt{2}} r_0 s_0^2\right) + \dfrac{\sqrt{3}}{2}\left(r_0^2 s_0 + \dfrac{1}{\sqrt{2}} r_0 s_0^2\right) + \sqrt{\dfrac{3}{8}}\, r_0^3 \\ Q_{yy} = 0 \\ Q_{zz} = -\dfrac{\sqrt{3}}{2}\left(r_0^2 s_0 + \dfrac{1}{\sqrt{2}} r_0 s_0^2\right) - \dfrac{\sqrt{3}}{2}\left(r_0^2 s_0 + \dfrac{1}{\sqrt{2}} r_0 s_0^2\right) - \sqrt{\dfrac{3}{8}}\, r_0^3 \end{cases} \tag{4}$$

from eqs 1 and 2 are also in the order of RuC_8-1 < RuC_8-2 < RuC_8-3 ≈ RuC_{24}-3. That is, the expansion of the ligands from RuC_8-1 to RuC_8-2 and RuC_8-3 ideally leads to the increase in HTP, although the calculation was done under the assumption that the ruthenium dopant has only one rigid conformation. In fact, RuC_8-2 and RuC_8-3 showed higher experimental HTP values than RuC_8-1.

In contrast, the calculation for the helicity tensor Q_{ij} also indicates that RuC_8-3 and RuC_{24}-3 have higher HTPs than RuC_8-2, while they showed lower HTPs in the experiment. The HTP of RuC_{24}-3 was lower than even RuC_8-1. As for this reason, we consider that the above hypothesis that ruthenium dopants align with nematic hosts by directing one of the elongated ligands to the local director is not satisfactory in the cases of RuC_8-3 and RuC_{24}-3. Triaxial RuC_8-3 and disk-like RuC_{24}-3 are probably poorly oriented along the director of MBBA. HTP is the product of the helicity tensor and ordering matrix (S_{ii}) (eq 2). Poor orientation leads to a low HTP value. We have designed the tris-chelate dopants expecting that one ligand directs to the alignment axis of the host liquid crystal molecules. Such a picture was confirmed in the case of uniaxial [Ru(acac)$_2$($L_{backbone}$)] by polarized absorption spectroscopy.[24] However, for RuC_8-3 and RuC_{24}-3 with isotropic structures, we consider that they are stabilized in liquid crystal media without directing one of the ligands to the director of the liquid crystal host. In particular, RuC_{24}-3 with nine alkoxy chains probably have various conformations in liquid crystal media.

On the contrary, we consider that RuC_8-2 with an anisotropic structure retained a balance of molecular helicity and good orientation. Biaxial RuC_8-2 may poorly orient in liquid crystals compared to RuC_8-1, while it is expected to exhibit higher molecular helicity than RuC_8-1. The previous report on Ru-*n* found that uniaxial rod structure was suitable for the acquisition of high HTPs in the case of the perpendicular type (Figure 1). However, the present study indicates that biaxial dopants show high HTPs at least in the case of the parallel type. To clarify the actual interaction between a biaxial metal complex dopant and liquid crystal molecules is important for the clear establishment of the structure-HTP relations in Δ, Λ chiral dopants. MD simulations for the system of MBBA doped with biaxial or triaxial Ru(III) complexes are currently underway.

dx.doi.org/10.1021/ic401240f | Inorg. Chem. 2013, 52, 11042−11050

CONCLUSIONS

The modification of one, two, and three ligands in the [Ru(acac)$_3$] core has been systematically performed to investigate the correlation between the molecular structure and HTP for a nematic liquid crystal. Five new Ru(III) complexes, [Ru(acac)$_2$(acacC_8)] (**RuC_8-1**, acacC_8 = 3-(4′-octyloxy-phenylalkynyl)-pentane-2,4-dionato), [Ru(acac)-(acacC_8)$_2$] (**RuC_8-2**), [Ru(acacC_8)$_3$] (**RuC_8-3**), [Ru(acacC_0)$_3$] (**RuC_0-3**, acacC_0 = 3-(phenylalkynyl)-pentane-2,4-dionato), and [Ru(acacC_{24})$_3$] (**RuC_{24}-3**, acacC_{24} = 3-(3′,4′,5′-tri-(octyloxy)-phenylalkynyl)-pentane-2,4-dionato) have been synthesized. Optical resolution by HPLC on a chiral column was possible for the complexes except for **RuC_0-3**. The presence of octyloxy groups improved the efficiency of the optical resolution. The HTPs of the Δ isomers of **RuC_8-1**, **RuC_8-2**, **RuC_8-3**, and **RuC_{24}-3** for a nematic liquid crystal, *N*-(4-methoxybenzilidene)-4-butylaniline (MBBA), were determined to be +60, +109, +78, and +41, respectively. Planar substituents (C_8 in this study) introduced to be aligned parallel with the C_2 axis of [Ru(acac)$_3$] core had the effect of inducing a right-handed helix (a positive HTP) common in every complex (vice versa for the Λ isomer), while the magnitude of the HTP was not simply proportional to the number of substituents. The calculation based on surface chirality model indicates that the molecular helix (helicity tensor Q_{ij}) increases in the order of **RuC_8-1** < **RuC_8-2** < **RuC_8-3** ≈ **RuC_{24}-3**. In contrast, low ordering (S_{zz}) toward a director of host liquid crystals was indicated for **RuC_8-3** and **RuC_{24}-3** because of their isotropic structures. Based on these results, we concluded that biaxial **RuC_8-2** shows high HTP because of a good balance of molecular helicity and high ordering. We believe that our results lead to the rational development of Δ, Λ chiral dopants, which were mainly confined to the uniaxial [Ru-(acac)$_2$($L_{backbone}$)] type.

ASSOCIATED CONTENT

Supporting Information

Listings of ESI-MS spectra, UV−vis spectrum, chromatograms in HPLC, calculation based on surface chirality model, crystal data, and X-ray crystallographic file in CIF format (CCDC 937697−937701). This material is available free of charge via the Internet at http://pubs.acs.org.

AUTHOR INFORMATION

Corresponding Author

*E-mail: yoshidaj@kitasato-u.ac.jp. Phone: +81-42-778-7980. Fax: +81-42-9953.

Notes

The authors declare no competing financial interest.

ACKNOWLEDGMENTS

This study was supported by a Kitasato University Research Grant for Young Researchers.

REFERENCES

(1) Solladié, G.; Zimmermann, R. G. *Angew. Chem., Int. Ed. Engl.* **1984**, *23*, 348−362.
(2) *Chirality in Liquid Crystals*; Kitzerow, H.-S., Bahr, C., Eds.; Springer-Verlag: New York, 2001.
(3) Maeda, K.; Takeyama, Y.; Sakajiri, K.; Yashima, E. *J. Am. Chem. Soc.* **2004**, *126*, 16284−16285.
(4) Eelkema, R.; Feringa, B. L. *J. Am. Chem. Soc.* **2005**, *127*, 13480−13481.
(5) Eelkema, R.; Feringa, B. L. *Org. Biomol. Chem.* **2006**, *4*, 3729−3745.
(6) Zahn, S.; Proni, G.; Spada, G. P.; Canary, J. W. *Chem.—Eur. J.* **2001**, *7*, 88−93.
(7) Kuball, H. −G.; Weib, B.; Beck, A. K.; Seebacb, D. *Helv. Chim. Acta* **1997**, *80*, 2507−2514.
(8) Braun, M.; Hahn, A.; Engelmann, M.; Fleischer, R.; Frank, W.; Kryschi, C.; Haremza, S.; Kürschner, K.; Parker, R. *Chem.—Eur. J.* **2005**, *11*, 3405−3412.
(9) Goh, M.; Akagi, K. *Liq. Cryst.* **2008**, *35*, 953−965.
(10) Frank, B. B.; Blanco, B. C.; Jakob, S.; Ferroni, F.; Pieraccini, S.; Ferrarini, A.; Boudon, C.; Gisselbrecht, J.-P.; Seiler, P.; Spada, G. P.; Diederich, F. *Chem.—Eur. J.* **2009**, *15*, 9005−9016.
(11) Li, Y.; Urbas, A.; Li, Q. *J. Am. Chem. Soc.* **2012**, *134*, 9573−9576.
(12) Allen, M. P. *Phys. Rev. E* **1993**, *47*, 4611−4614.
(13) Cook, M. J.; Wilson, M. R. *J. Chem. Phys.* **2000**, *112*, 1560−1564.
(14) Wilson, M. R.; Earl, D. J. *J. Mater. Chem.* **2001**, *11*, 2672−2677.
(15) Wilson, M. R. *Chem. Soc. Rev.* **2007**, *36*, 1881−1888.
(16) Drake, A. F.; Gottarelli, G.; Spada, G. P. *Chem. Phys. Lett.* **1984**, *110*, 630−633.
(17) Anzai, N.; Machida, S.; Horie, K. *Chem. Lett.* **2001**, *30*, 888−889.
(18) Anzai, N.; Machida, S.; Horie, K. *Liq. Cryst.* **2003**, *30*, 359−366.
(19) Sato, H.; Sato, F.; Yamagishi, A. *Chem. Commun.* **2013**, *49*, 4773−4775.
(20) Hoshino, N.; Matsuoka, Y.; Okamoto, K.; Yamagishi, A. *J. Am. Chem. Soc.* **2003**, *125*, 1718−1719.
(21) Matsuoka, Y.; Sato, H.; Yamagishi, A.; Okamoto, K.; Hoshino, N. *Chem. Mater.* **2005**, *17*, 4910−4917.
(22) Yoshida, J.; Sato, H.; Yamagishi, A.; Hoshino, N. *J. Am. Chem. Soc.* **2005**, *127*, 8453−8456.
(23) Furuno, Y.; Sato, H.; Yoshida, J.; Hoshino, N.; Fukuda, Y.; Yamagishi, A. *J. Phys. Chem. B* **2007**, *111*, 521−526.
(24) Yoshida, J.; Sato, H.; Hoshino, N.; Yamagishi, A. *J. Phys. Chem. B* **2008**, *112*, 9677−9683.
(25) Ferrarini, A.; Moro, G. J.; Nordio, P. L. *Phys. Rev. E* **1996**, *53*, 681−688.
(26) Ferrarini, A.; Nordio, P. L. *J. Chem. Soc., Perkin Trans. 2* **1998**, 455−460.
(27) Matteo, A.; Todd, S. M.; Gottarelli, G.; Solladie, G.; Williams, V. E.; Lemieux, R.; Ferrarini, A.; Spada, G. P. *J. Am. Chem. Soc.* **2001**, *123*, 7842−7851.
(28) Pieraccini, S.; Donnoli, M. I.; Ferrarini, A.; Gottarelli, G.; Licini, G.; Rosini, C.; Superchi, S.; Spada, G. P. *J. Org. Chem.* **2003**, *68*, 519−526.
(29) Celebre, G.; Luca, G. D.; Maiorino, M.; Iemma, F.; Ferrarini, A.; Pieraccini, S.; Spada, G. P. *J. Am. Chem. Soc.* **2005**, *127*, 11736−11744.
(30) Pieraccini, S.; Masiero, S.; Ferrarini, A.; Spada, G. P. *Chem. Soc. Rev.* **2011**, *40*, 258−271.
(31) Kakegawa, N.; Hoshino, N.; Matsuoka, Y.; Wakabayashi, N.; Nishimura, S.; Yamagishi, A. *Chem. Commun.* **2005**, 2375−2377.
(32) Matsumura, K.; Iwayanagi, S. *Oyo Butsuri* **1974**, *43*, 126.
(33) Long, Y.; Chen, H.; Yang, Y.; Wang, H.; Yang, Y.; Li, N.; Li, K.; Pei, J.; Liu, F. *Macromolecules* **2009**, *42*, 6501−6509.
(34) Endo, A.; Shimizu, K.; Sato, G. P.; Mukaida, M. *Chem. Lett.* **1985**, 581−584.
(35) Kasahara, Y.; Hoshino, Y.; Kajitani, M.; Shimizu, K.; Sato, G. P. *Organometallics* **1992**, *11*, 1968−1971.
(36) Sheldrik, G. M. *Acta Crystallogr. A* **2008**, *64*, 112−122.
(37) Spek, A. L. *J. Appl. Crystallogr.* **2003**, *36*, 7−13.
(38) Frisch, M. J.; Trucks, G. W.; Schlegel, H. B.; Scuseria, G. E.; Robb, M. A.; Cheeseman, J. R.; Montgomery, Jr., J. A.; Vreven, T.; Kudin, K. N.; Burant, J. C.; Millam, J. M.; Iyengar, S. S.; Tomasi, J.; Barone, V.; Mennucci, B.; Cossi, M.; Scalmani, G.; Rega, N.; Petersson, G. A.; Nakatsuji, H.; Hada, M.; Ehara, M.; Toyota, K.; Fukuda, R.; Hasegawa, J.; Ishida, M.; Nakajima, T.; Honda, Y.; Kitao, O.; Nakai, H.; Klene, M.; Li, X.; Knox, J. E.; Hratchian, H. P.; Cross, J. B.; Bakken, V.; Adamo, C.; Jaramillo, J.; Gomperts, R.; Stratmann, R.

E.; Yazyev, O.; Austin, A. J.; Cammi, R.; Pomelli, C.; Ochterski, J. W.; Ayala, P. Y.; Morokuma, K.; Voth, G. A.; Salvador, P.; Dannenberg, J. J.; Zakrzewski, V. G.; Dapprich, S.; Daniels, A. D.; Strain, M. C.; Farkas, O.; Malick, D. K.; Rabuck, A. D.; Raghavachari, K.; Foresman, J. B.; Ortiz, J. V.; Cui, Q.; Baboul, A. G.; Clifford, S.; Cioslowski, J.; Stefanov, B. B.; Liu, G.; Liashenko, A.; Piskorz, P.; Komaromi, I.; Martin, R. L.; Fox, D. J.; Keith, T.; Al-Laham, M. A.; Peng, C. Y.; Nanayakkara, A.; Challacombe, M.; Gill, P. M. W.; Johnson, B.; Chen, W.; Wong, M. W.; Gonzalez, C.; and Pople, J. A. *Gaussian 03*, Revision C.02; Gaussian, Inc.: Wallingford, CT, 2004.

(39) **RuC$_8$-2** and **RuC$_8$-3** are elongated parallel to the molecular C_2 axes. In contrast, several of ***Ru-n*** which have biaxial structures are elongated perpendicular to the molecular C_2 axis.

(40) Kashiwara, S.; Takahashi, M.; Nakata, M.; Taniguchi, M.; Yamagishi, A. *J. Mater. Chem.* **1998**, *8*, 2253−2257.

(41) Kobayashi, H.; Matsuzawa, H.; Kaizu, Y.; Ichida, A. *Inorg. Chem.* **1987**, *26*, 4318−4323.

(42) Koiwa, T.; Masuda, Y.; Shono, J.; Kawamoto, Y.; Hoshino, Y.; Hashimoto, T.; Natarajan, K.; Shimizu, K. *Inorg. Chem.* **2004**, *43*, 6215−6223.

(43) Saeva, F. D.; Sharpe, P. E.; Olin, G. R. *J. Am. Chem. Soc.* **1973**, *95*, 7656−7659.

(44) Sackmann, E.; Voss, J. *Chem. Phys. Lett.* **1972**, *14*, 528−532.